1/35

THE EFFECT OF VEGETATION ON INFILTRATION IN SHALLOW SOILS UNDERLAIN BY FISSURED BEDROCK

Prepared for

Nuclear Regulatory Commission
Contract NRC-02-93-005

Prepared by

Stuart A. Stothoff
Dani Or (Consultant)
David P. Groeneveld (Consultant)
Scott B. Jones

Center for Nuclear Waste Regulatory Analyses
San Antonio, Texas

July 1997

ABSTRACT

Field and modeling studies are performed to achieve insight into the hydrologic behavior of a semi-arid environment characterized by shallow, permeable soils overlying a bedrock with soil-filled fissures. Particular attention is given to the impact of vegetation on the hydrologic system. Field investigations suggest that widely spaced soil-filled fissures are conducive to plant growth even when fissure are burried below soils as deep as 30 cm. This conclusion is based on lines of evidence including linear plant-growth features observed on aerial photographs, comparisons of plant cover within the fissured environment to plant cover in comparable environments lacking the fissures, and observations from excavations. Based on the explicit simulation of individual plant roots for a newly germinated plant over a growing season, it is concluded that the fissure environment provides a competitive advantage. Therefore, plants that germinate above a fissure are more likely to survive, thereby developing linear features above fissures. Modeling studies examining the impact of plant transpiration on a system with shallow soil, sloping bedrock, and discrete fissures suggest that transpiration may strongly limit net infiltration; significant infiltration, however, can occur when plants are dormant, and therefore most infiltration would be expected to occur during winter.

3/35

CONTENTS

Section Page

1 INTRODUCTION 1-1

2 BACKGROUND 2-1
2.1 GEOLOGIC SETTING 2-1
2.2 SURFICIAL DEPOSITS AND FRACTURE FILLINGS 2-1
2.3 HYDROLOGIC CONSIDERATIONS 2-3

3 FIELD INVESTIGATION OF VEGETATIVE PATTERNS 3-1
3.1 EXPERIMENTAL METHODS 3-1
3.2 VEGETATION COVER AND COMPOSITION 3-1
3.3 EXPERIMENTAL EVIDENCE FOR PLANT-FISSURE INTERACTIONS 3-3

4 SIMULATIONS OF ROOT GROWTH INTO FISSURES 4-1
4.1 METHODS 4-1
4.2 RESULTS 4-2

5 LANDSCAPE-SCALE HYDROLOGIC SIMULATIONS 5-1
5.1 METHODS 5-1
5.2 RESULTS 5-1

6 SUMMARY AND CONCLUSIONS 6-1

7 REFERENCES 7-1

4/35

FIGURES

Figure		Page
2-1	Location of Yucca Mountain, Nevada	2-2
2-2	Schematic of hydrologic behavior of the caprock	2-4
3-1	Location of a linear vegetation feature in the caprock of Yucca Crest: (a) aerial view, (b) closeup of linear feature, and (c) excavated fissure in bedrock	3-4
4-1	Root systems resulting from 100-day growth, overlain into one plot	4-5
5-1	Model domain for investigation of flow into fissures	5-2
5-2	Water-flux response in fissures following a 100-mm precipitation event: (a) top of soil filling without plant uptake; (b) bottom of soil filling without plant uptake; (c) top of soil filling with plant uptake, and (d) bottom of soil filling with plant uptake.	5-5
5-3	Water-flux response in fissures following a 30-mm precipitation event: (a) top of soil filling without plant uptake; (b) bottom of soil filling without plant uptake; (c) top of soil filling with plant uptake; and (d) bottom of soil filling with plant uptake	5-6
5-4	Water-content distributions 9 days after a 30-mm rainfall event: (a) without plants, and (b) with plants	5-7

5/35

TABLES

Table Page

3-1 Average LAI and fraction cover of perennial plant species (nomenclature and authorities following Hickman (1995) measured at five locations on slopes dominated by crystal-rich tuff. Affinity refers to species generally found in the Great Basin (G) or Mojave Desert (M). 3-2

3-2 Mean perennial plant cover on Yucca Mountain, Nevada, measured on high-resolution air photos 3-3

4-1 Hydraulic parameters for the porous media used in seedling simulation studies 4-2

4-2 Parameters describing plant and root growth used in root-growth simulations. Functions are linearly interpolated between extremes and held constant outside of specified ranges. 4-3

5-1 Hydraulic parameters for the porous media used in landscape hydraulic simulations studies 5-3

5-2 Cumulative flux (mm) passing fissure center during the 30 days including and following the rainfall event. Negative values denote downward flux. 5-4

6/35

ACKNOWLEDGMENTS

This paper was prepared to document work performed by the Center for Nuclear Waste Regulatory Analyses (CNWRA) for the NRC under Contract No. NRC-02-93-005. The activities reported here were performed on behalf of the NRC Office of Nuclear Material Safety and Safeguards, Division of Waste Management. The paper is an independent product of the CNWRA and does not necessarily reflect the views or regulatory position of the NRC. The authors would like to acknowledge the suggestions and comments made by Gordon Wittmeyer and Budhi Sagar, which tremendously improved the quality of the paper.

QUALITY OF DATA, ANALYSES, AND CODE DEVELOPMENT

DATA: CNWRA-generated data contained in this report have been documented according to quality assurance requirements described in the CNWRA Quality Assurance Manual. Sources for other data should be consulted for determining the level of quality for those data.

ANALYSES AND CODES: Neither the HYDRUS-2D simulator nor the root-growth simulator is configured under the CNWRA's Software Configuration Procedure. At present, the CNWRA does not anticipate the use of either of these codes for regulatory reviews.

1 INTRODUCTION

Yucca Mountain (YM), Nevada, is the potential site of a geologic repository for high-level radioactive waste. YM is located approximately 160 km northwest of Las Vegas, NV, comprises a sequence of fractured welded and nonwelded tuffs, has an unsaturated zone up to 750 m thick, and has a mean annual precipitation (MAP) of 150 to 170 mm. YM is located within the transition zone between the Mojave Desert and the Great Basin Desert. The potential repository is currently designed to be located within a fractured, densely welded tuff layer approximately 250 m above the water table. Numerous assessments of the expected performance of the potential repository have identified the magnitude of deep percolation fluxes past the repository horizon as a critical factor in the potential-repository performance (Nuclear Regulatory Commission, 1992, 1995; Electric Power Research Institute, 1990, 1992, 1996; Eslinger et al., 1993; Sandia National Laboratories, 1992, 1994; Andrews et al., 1994; TRW Environmental Safety Systems, Inc., 1995). In turn, the magnitude of deep percolation fluxes is strongly dependent on the magnitude of net infiltration below the zone of evapotranspiration, providing strong motivation for studying and quantifying infiltration processes in the YM area.

Numerous studies have examined infiltration processes in the vicinity of YM. Flint et al. (1994) present a conceptual model of shallow-infiltration processes at YM that is in general agreement with available data and modeling studies presented by Long and Childs (1993) and Stothoff (1997). The studies suggest that mean annual infiltration (MAI) may be relatively high on ridgetops and sideslopes (due to accessible bedrock fractures), relatively low in deep alluvium (due to large soil-water storage capacity and plant uptake), and may be locally enhanced near ephemeral channels due to flow concentration. The trend toward greater MAI where shallow soils overlie fractured bedrock is suggested by disparate lines of evidence including geothermal heat-flux-anomaly analysis (Sass et al., 1988), bomb-pulse and natural tracers (Fabryka-Martin et al., 1996), and neutron-probe readings (Flint and Flint, 1995). The various indications that distributed recharge may be significant, with an areal average that may dominate concentrated recharge from ephemeral channels, suggest that recharge behaves somewhat differently than expected for arid and semiarid environments. The apparent anomaly provides motivation for studying flow processes in shallow soils (particularly in view of the sensitive response of potential-repository performance measures to net infiltration).

Deep recharge in arid and semiarid environments has been studied by various researchers [e.g., Allison and Hughs (1978); Allison et al. (1994); Barnes et al. (1994); Conrad (1993); Gee et al. (1994); Nichols (1987); Phillips (1994); Scanlon (1991, 1992; Tyler and Walker (1994)], and hydrologic interactions in deep soil profiles are reasonably well understood. Deep recharge is determined by the interaction of the spatial and temporal distributions of precipitation with evapotranspiration. Estimates of recharge in deep alluvium profiles near YM range from 8 to less than 0.01 mm/yr (Tyler and Walker, 1994), corresponding to roughly 5 to less than 0.01 percent of the long-term average precipitation of 150 mm/yr at the elevation studied. In the absence of vegetation, surface runon-runoff processes and bare-soil evaporation determine the fraction of precipitation resulting in net recharge. Where vegetation is present, plant water uptake may consume a large portion of the precipitation (Gee et al., 1994; Tyler and Walker, 1994).

Hydrologic interactions have been less studied in shallow soils underlain by fractured bedrock, as is found on the crest and sideslopes of YM. Approximately 60 percent of the ground surface above the potential repository footprint is characterized by fractured welded tuff, either exposed or overlain by soils (i.e., unconsolidated porous materials) generally less than 50 cm in depth. The low soil-water storage capacity and plentitude of fractures can result in rapid transmission of infiltrating waters to well below

8/35

the top of the bedrock, as evidenced by rapid responses in neutron-probe data (Flint et al., 1994; Flint and Flint, 1995), and bomb-pulse ^{36}Cl hundreds of meters into the bedrock (Fabryka-Martin et al., 1996). Once within the fractured bedrock, water would be expected to be minimally available for plant uptake. However, even with limited soil-water storage, there is well-established perennial (and annual) vegetation cover on these surfaces. In areas with exposed bedrock and very shallow soils (less than 10 cm), vegetation is established in cracks and fissures. In areas with well-separated fissures and deeper soils (several tens of centimeters), vegetation often follows linear patterns suggestive of rooting into bedrock fissures. In soils unconstrained by bedrock and associated fissures, plant-root density, and by analogy plant uptake, is commonly modeled as decaying approximately exponentially with depth (Gerwitz and Page, 1974; Campbell, 1985; Fayer and Jones, 1990). Plant root distributions and water uptake under the constraints of shallow soils and fissured bedrock have not been well established and are of direct interest for quantifying net shallow infiltration at YM.

Three general types of shallow-soil environments are predominant at YM: (i) the crystal-rich caprock environment, with widely spaced fissures, relatively verdant vegetation, and relatively shallow slopes; (ii) the crystal-poor welded-tuff environment, with frequent carbonate-filled cooling joints, relatively sparse vegetation, and relatively steep slopes; and (iii) the scree or talus environment, with no plants within the scree, relatively verdant vegetation bordering the scree, and slopes of 30 to 60 percent. In this study, the caprock environment is examined in detail. Due to the relatively shallow slopes in the caprock environment, it is most accessible to field observation and may be most amenable to modeling studies. Further, borehole and modeling studies (Flint and Flint, 1995; Fabryka-Martin et al., 1996; Long and Childs, 1993; Bagtzoglou et al., 1996) strongly suggest that MAI is significant within this environment. Little or no field evidence of infiltration processes has been gathered in the relatively inaccessible sideslope environments to date, except at the extreme bottom and top of the slopes.

Factors influencing hydrologic processes in the caprock environment are examined here using a combination of techniques. The caprock environment exhibits linear patterns of vegetation in aerial photographs even where the bedrock is covered with soil which is suggestive of rooting within fissures. Types of perennial vegetation present in the environment and field observations of rooting patterns in a linear feature are discussed in chapter 3. The observed plentitude of roots within fissures and the presence of a fissure below the linear feature suggests that fissures provide a competitive advantage to perennial plants for soil depths to at least 30 cm. Hypothesizing that the competitive advantage must be realized at the early stages of growth, a three-dimensional (3D) modeling exercise is described in chapter 4 that simulates the growth of individual roots and soil-water uptake for a generic plant in the vicinity of a single fissure. The exercise is intended to investigate an explicit-simulation method for extracting plant-root distributions in soils and fissures. The modeling exercise suggests that the fissure does indeed offer a competitive advantage; interestingly, water is extracted from the bedrock interface as well as the soil. Finally, a two-dimensional (2D) modeling approach considering transpiration, lateral flow, and several fissures on a landscape scale is presented in chapter 5, and the impact of vegetation on net infiltration for typical rainfall events is examined. Conclusions from the study are discussed in chapter 6. The study is intended to ultimately provide input to modeling exercises that assess the performance of the potential repository.

2 BACKGROUND

2.1 GEOLOGIC SETTING

The proposed repository, shown in figure 2-1, is currently designed to be located in fractured, densely welded tuff approximately 250 m above the water table. The repository footprint, with an area of approximately 3 km^2, is overlain by as much as 500 m of welded and nonwelded tuff units that dip 5 to 10 degrees to the east. The west face of YM was formed by the steeply dipping north-trending Solitario Canyon fault. Within the repository footprint east of Yucca Crest, the tuff sequence is deeply dissected by washes cut into the welded Tiva Canyon unit of the Paintbrush Formation. Alluvial deposits in the washes can be several meters deep within the footprint and tens to hundreds of meters deep within a few kilometers of YM. On sideslopes and ridgetops within the repository footprint, shallow surficial deposits (called soils herein for simplicity of nomenclature) cover the fractured and fissured bedrock to depths typically less than 50 cm. Scree and talus deposits occur on steep sideslopes and can extend to depths greater than 1 m.

Tiva Canyon tuff, comprising several units of moderately to densely welded tuff, forms the bulk of the outcrop bedrock atop the potential-repository footprint. The units can be grouped into crystal-rich and crystal-poor tuffs (Buesch et al., 1996). The crystal-rich units overlie the crystal-poor units and tend to form an erosion-resistant layer that we refer to generically as caprock. The crystal-rich units form relatively massive blocks, with few cooling joints within a block but soil-filled fissures between blocks. The crystal-poor units are less resistant to erosion due to numerous cooling joints (typically carbonate-filled near the soil-bedrock interface), tend to be dissected into relatively steep washes atop the potential-repository footprint, and are overlain by scree or talus on portions of the steeper slopes. The focus of the current investigation is on the hydrologic behavior of the crystal-rich caprock forming much of the ridgetop environments at YM, particularly aspects of the hydrologic behavior affected by vegetation growing within the soil-filled fissures. Areas in which crystal-rich Tiva Canyon units outcrop are shown in figure 2-1.

Flint et al. (1996) report typical saturated hydraulic conductivity values, based on 83 outcrop samples, of about 10^{-3} cm hr^{-1} for bedrock units that we consider as lying within the caprock environment. Core samples from boreholes penetrating the same units suggest that bedrock in this environment may have two sets of values, with means on the order of 10^{-2} cm hr^{-1} and 5×10^{-7} cm hr^{-1} (Flint, 1996). For comparison, the densely welded crystal-poor units tend to have saturated hydraulic conductivities in the range of 10^{-4} to 10^{-6} cm hr^{-1} (Flint, 1996).

2.2 SURFICIAL DEPOSITS AND FRACTURE FILLINGS

The mildly sloping caprock surface is overlain by loamy sand soil of variable thickness, from exposed caprock to depths of about 0.5 m. Soil texture varies with depth from loamy sand to loam, typically features a light desert pavement at the surface, and exhibits occasional embedded rock shards and fragments at all depths. The fine-content composition (<2 mm) is remarkably spatially uniform on YM. Schmidt (1989) reports sand, silt, and clay contents of 60.8, 26.1, and 13.2 percent by weight, respectively, and corresponding standard deviations of 5.38, 5.18, and 4.66 percent. Schmidt (1989) found that the gravel component (<75 mm) of the soil is 45.1 percent by weight, with a standard deviation of 9.63. Our limited confirmatory analyses show average sand, silt, and clay contents of 66.4, 24.3, and 9.3 percent by weight, respectively, with corresponding standard deviations of 5.29, 3.73, and 2.99, and

10/35

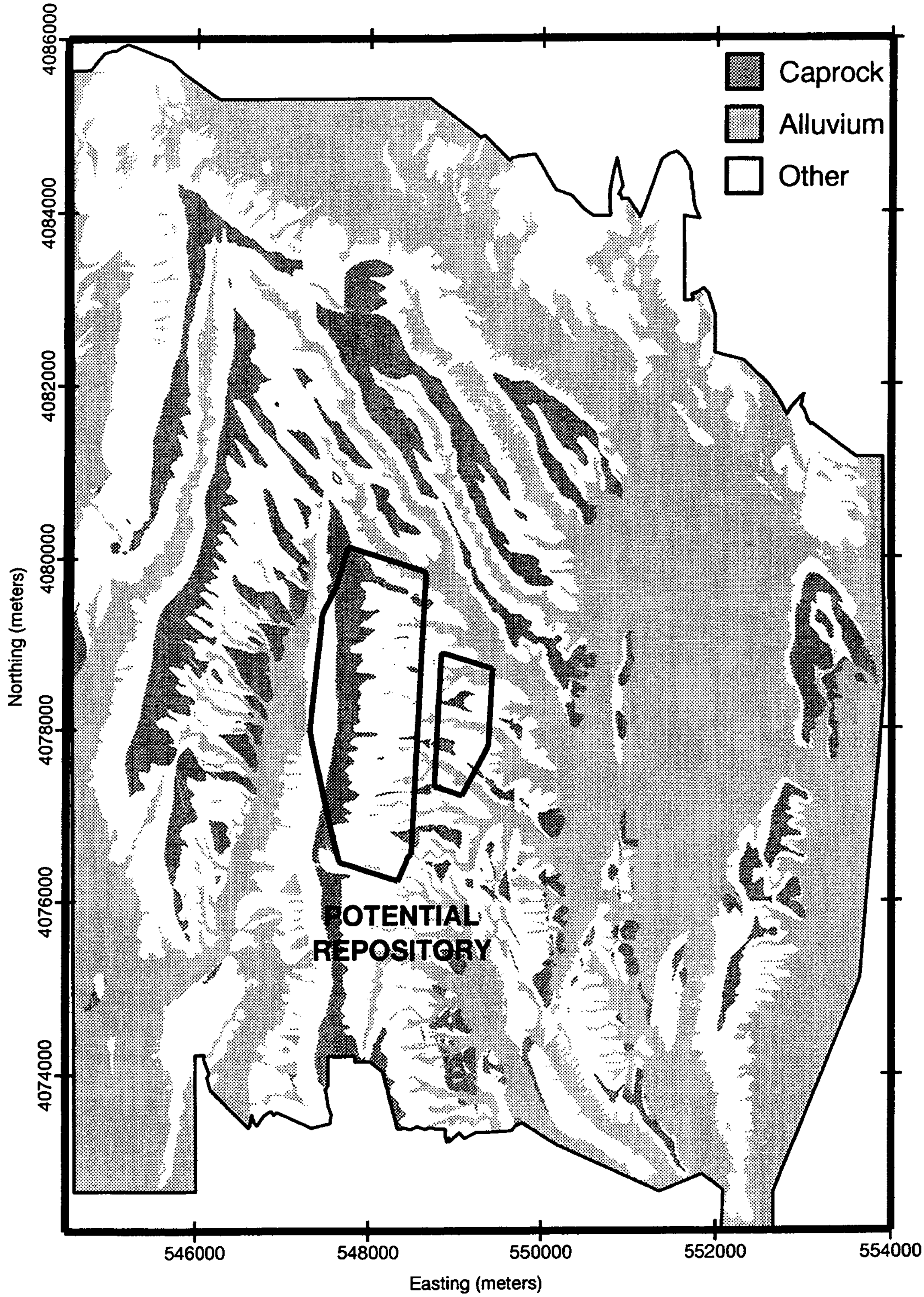

Figure 2-1. Location of Yucca Mountain, Nevada

electrical conductivity of about 0.4 mmho cm^{-1} for all 33 samples. Based on a soil texture analysis, Schmidt (1989) estimated the saturated hydraulic conductivity of the fine components to be about 2 cm hr^{-1}. Several ponded-head permeameter measurements performed by the authors at scattered locations provided results consistently in the range of 10 to 18 cm hr^{-1}. The Schmidt, (1989) analysis included samples from the caprock, sideslopes, and alluvium-filled washes, while our analyses included only samples from caprock and sideslope environments.

Fine-textured fill, ranging from loam at the soil-rock interface to various forms of calcite (Quade and Cerling, 1990) at larger depths, is prevalent within fissures in crystal-rich Tiva Canyon caprock. Detailed analysis of the origin of the surface loamy sand soil and the sandy loam to loam filling the top portions of the fissures is beyond the scope of the study. However, based on the mineralogy and texture of these soils, their position in the landscape (top of the mountain crest), and the large loess deposits forming the fine component of the soils in nearby Amargosa Valley, it is reasonable to assume that these deposits are probably aeolian. The uniform consistency of the fine components of the soils overlying various types of bedrock is confirmatory evidence for an aeolian origin. The source of the calcite is a matter of an ongoing debate; however, Quade and Cerling (1990) provide evidence that it is pedogenic.

2.3 HYDROLOGIC CONSIDERATIONS

Plant-fissure interactions on Yucca Crest involve an array of hydrologic processes that are accentuated by the low storage capacity of the overlying soil, on the one hand, and focussed flows into and through fissures in the underlying bedrock, on the other. Other hydrologic processes also may occur, such as lateral flow at soil-bedrock interfaces and overland flow following heavy rainstorms. A schematic surface profile with the primary hydrologic processes under consideration is depicted in figure 2-2.

In water-limited ecosystems such as the YM area, it is thought that vegetation density and patterns are controlled by the distribution and availability of soil water (Noy-Meir, 1973); Fonteyn and Marshall, 1981). Stephenson (1990) has shown that the (local) water balance is the single most important factor in explaining vegetation patterns in many ecosystems. Root growth into bedrock fissures has been studied in similar arid (Herwitz and Olsvig-Whittaker, 1989) and semiarid (Zwieniecki and Newton, 1995) ecosystems. Based on these studies, and on the polygon-like vegetation patterns on Yucca Crest (and similar nearby landscape units), we hypothesize that near-surface hydrologic processes interact with widely spaced fissures in the bedrock to provide conditions that enhance plant growth along the fissures. The role of vegetation in intercepting slowly moving water within fissures is of particular interest for deep recharge predictions at YM.

The fine-textured fill within fissures is a critical feature of hydrologic interactions in crystal-rich Tiva Canyon caprock. Fine-textured fill not only helps in retaining a portion of the water feeding the fissure from above (thereby adding to the storage capacity available to roots), but also provides hydraulic continuity necessary for potential use of water held in bedrock pores (Zwieniecki and Newton, 1995). Because evaporation takes place at much slower rates for deep fissures than from near-surface soil layers, soil water storage in fissures can provide a means for survival of perennial vegetation during dry periods. Several caprock fissures are illustrated in figure 2-2. The left and right shrubs in figure 2-2 are examples of plants dominated by interactions with fissures. There is evidence, however, that widely spaced fissure-independent plants can also be established in relatively deep pockets of soil (center shrub in figure 2-2), with the shrub relying on the water-storage capacity of the soil.

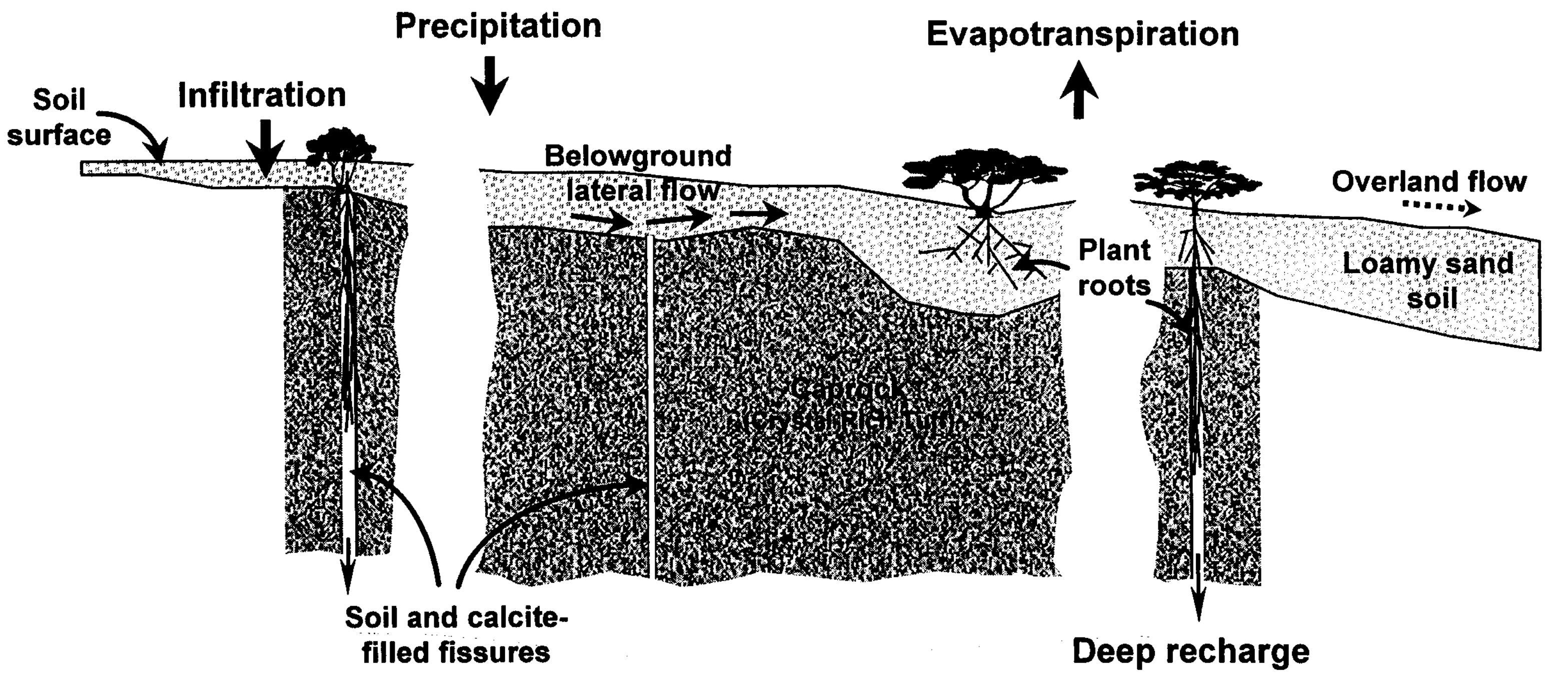

Figure 2-2. Schematic of hydrologic behavior of the caprock

Our hypothesis regarding the importance of fissures for supporting plant growth is supported by the disparity between relatively high vegetation density and low soil water storage capacity in the caprock environment. Typical and extreme soil depths overlying the crystal-rich tuff are 0.2 and 0.6 m., respectively. Ratliff et al., (1983) estimate the difference between field capacity and wilting point as $0.15m^3\ m^{-3}$, the plant-available soil water storage capacities would be about 30 and 90 mm, respectively. Even when minimal transpiration rates of less than 0.1 mm/day are considered, the competing process of soil evaporation at relatively low rates of 1 mm/day (Evans et al., 1981) would have depleted the plant-available soil water from the 0.2-m soil profile within a month. Hence, we postulate that plants must rely on other, longer-term soil-water sources such as found in sediment-filled fissures in the caprock for areas with typical soil depths. The possibility of reliance on soil storage cannot be ruled out, however, in the deeper soil profiles of the caprock environment.

The lateral-flow processes shown in figure 2-2 are expected to be locally significant in the caprock environment, focussing water into fissures and drawing water toward plants. Due to the relatively shallow slopes, prevalent bedrock fissuring, and numerous plants, it is anticipated that subsurface lateral flow rarely occurs over distances significantly larger than a few meters. Overland flow in the YM caprock environment should be minimal. Soils at YM are sufficiently permeable, even if the hydraulic conductivity is as low as 2 cm hr^{-1} as obtained from the texture analysis, that they should accept water at most rainfall rates until the wetting front contacts bedrock (a total influx of 3 to 9 cm for the soil depths discussed above). Overland flow may still be inhibited after the soil storage capacity is exceeded if soil water can quickly escape to depth within fissures. Overland flow would be expected to occur in areas with shallow-to-nonexistent soils, thereby concentrating the water into exposed fissures and downslope areas. Soils in the caprock area tend to deepen downslope (increasing storage capacity) so that the lateral extent of overland flow would be expected to be limited. In confirmation of these qualitative observations, geomorphic evidence for overland flow (such as erosive rills) is scarce in areas in which caprock is the bedrock material.

3 FIELD INVESTIGATION OF VEGETATIVE PATTERNS

3.1 EXPERIMENTAL METHODS

In approaching this study, we realized at the outset that the crystal-rich caprock provided a relatively favorable location for plant growth in comparison to locations downslope in which the tuff was less resistant. The caprock comprises relatively broad, gently sloping physiognomy that contrasts to the dissected arroyos comprising the stratigraphically deeper and less resistant tuff. Caprock-dominated environments exhibit occasional relatively deep (20 to 50 cm) pans filled with soil. These sites may perch water and, thus, foster greater vegetation cover than on locations of less resistant tuff that has similar aspect and slope and position just downslope and to the east of the caprock. The less resistant tuff generally has less soil cover as well (often 15 cm in depth or less). Perennial-vegetation measurements were obtained to document the relative richness of the caprock environment for vegetation. Annual species, which fluctuate greatly according to winter rainfall, were not recorded.

Vegetation was measured in the field at five locations on the crystal-rich tuff using the line point-quadrat technique (Heady et al., 1959). For this technique, sharpened pins were lowered vertically through the canopy at set intervals, using 50-m tape stretched across the vegetation of interest. Contacts of the sharpened tips of pins (regarded as dimensionless (Goodall, 1952) with the leaves of plants were recorded. Leaf area index (LAI), that is the area of leaves per area of ground, was calculated by dividing total leaf contacts by the number of pins used on the transect, then multiplying by two to account for an extinction factor due to spherical leaf distribution (Groeneveld, 1997). Cover was calculated by dividing the total number of pins that penetrated canopies, either hitting or missing leaves, by the total number of pins used on the transect. These transects were obtained on March 26 and 30, 1997, prior to expected total leafout of the vegetation generally occurring during about mid-May (Leary, 1990).

Vegetation cover was also evaluated by photogrammetry on low-altitude, high-resolution vertical color-print air photographs of the repository block. For this analysis, approximately 30 m^2 homogeneous patches of vegetation on uniform slopes were chosen and overlaid with a template that delimited a grid field of 505 points. Perennial plant canopies underlying grid points were tallied. The frequency of these tallies versus the total number of grid points yields a measure of canopy cover equivalent to total perennial vegetation cover measured by line-point transect; however, since a larger number of transects and concomitantly larger number of points can be obtained on the air photographs, the photogrammetric technique is statistically more robust. Hence, the line-point transects obtained in the field provide an estimate of species composition while the photogrammetric data were used to provide comparison between locations in which the hydrology was dominated by crystal-rich caprock and locations in which the substrate was derived from less resistant crystal-poor tuff.

3.2 VEGETATION COVER AND COMPOSITION

The perennial vegetation of the crystal-rich caprock tuff on YM is transitional between Great Basin and Mojavean flora but is dominated by species more typical of the Great Basin (table 3-1). The measurements were obtained during late March, well in advance of the expected peak seasonal LAI; therefore, the overall observed LAI of 0.549 is less than the peak. In contrast, the cover developed in the field would not be expected to change through the season since the perennial plant canopies are persistent.

Table 3-1. Average LAI and fraction cover of perennial plant species (nomenclature and authorities following Hickman (1995) measured at five locations on slopes dominated by crystal-rich tuff. Affinity refers to species generally found in the Great Basin (G) or Mojave Desert (M).

Affinity	Species (Authority)	Family	LAI	Cover
G	Eriogonum fasciculatum (Benth.) Torrey & A. Gray	Polygonaceae	0.0745	0.068
G	Grayia spinosa Moq (Hook.)	Chenopodiaceae	0.145	0.064
G	Ericameria cooperi (A. Gray) H.M. Hall	Asteraceae	0.125	0.038
G	Chrysothamnum teretifolius (Durand & Hilg.) H.M. Hall	Asteraceae	0.063	0.030
G	Ephedra nevadensis S. Watson	Ephedraceae	0.039	0.028
M	Lycium andersonni A. Gray	Solanceae	0.008	0.026
M	Ephedra viridis Cov.	Ephedracae	0.027	0.018
M	Hymenoclea salsola A. Gray	Asteraceae	0.020	0.016
G	Ericameria linearifolia (DC.) Urb. & J. Wussow	Asteraceae	0.024	0.014
G	Krasheninnikovia lanata (Pursh) A.D.J. Meeuse & Smit	Chenopodiaceae	0.024	0.010
G	Atriplex confertifolia (Torrey & Fremont) S. Watson	Chenopodiaceae	0.0	0.008
G	Atriplex canescens (Pursh) Nutt.	Chenopodiaceae	0.0	0.006
G	Achnatherum speciosum (Trin. & Rupr.) Barkworth	Poaceae	0.0	0.004
Total			0.549	0.330

Table 3-2 presents the results from air photo interpretation of vegetation cover on crystal-rich caprock compared to locations on crystal-poor tuff that include ridgelines and north- and south-facing slopes. Aspect is an important predictor of vegetation cover on steeper slopes at YM; north- and south-facing aspects of the crystal-poor tuff have significantly different vegetation cover. This different cover is probably the result of increased evaporation on south-facing slopes due to greater insolation. North-facing slopes are dominated by the Great Basin species while south-facing slopes are dominated by Mojavean flora.

The crystal-poor ridgelines had approximately the same aspect and slope as the crystal-rich caprock and were found to support vegetative cover only slightly greater than the south-facing aspects. Significantly higher vegetation cover exists on the caprock-derived over the noncaprock-derived ridgelines, despite the similar aspect and slope. These data indicate the promotional effect of the increased soil accumulation and rooting volume in the caprock environment. In addition, soil-filled fissures in the caprock environment may provide significantly more plant-accessible water storage than the carbonate-filled cooling joints prevalent in the crystal-poor ridgelines.

Table 3-2. Mean perennial plant cover on Yucca Mountain, Nevada, measured on high-resolution air photos

Landscape Position	Rock Type	No. Samples	Cover (STD*)
Crest	Crystal-rich tuff	32	0.296 (0.037)
North aspects	Crystal-poor tuff	19	0.322 (0.086)
South aspects	Crystal-poor tuff	19	0.142 (0.032)
Ridgelines	Crystal-poor tuff	8	0.184 (0.027)
*Standard deviation of estimated plant cover			

3.3 EXPERIMENTAL EVIDENCE FOR PLANT-FISSURE INTERACTIONS

Of particular interest are those situations in which the spacing between adjacent fissures is larger than the extent of a typical rooting zone and the soil cover is too shallow to provide sufficient soil-water storage for vegetation. These conditions are likely to be conducive to alignment of vegetation along fissures. Such linear-like vegetation features should be observable on areal photographs. To test this hypothesis, we analyzed high-resolution air photographs and identified several prospective sites with linear-like vegetation alignment. One such site is depicted in figure 3-1. The soil was excavated at two locations between plants along a linear vegetation feature (figure 3-1a) to expose the bedrock, revealing a large fissure (0.05 to 0.15 m in aperture) aligned with the vegetation (figures 3-1b and c). As not all perennial vegetation on the crest lies within a linear or polygonal feature, other forms of adaptation must also be taking place, such as: (i) exploitation of fissures by lateral growth of roots into fissures (as discussed in chapter 4); and (ii) exploitation of soil bowls, due to irregularities in the caprock surface, that provide sufficient soil-water storage for plant growth. A confirmation of the latter mechanism was obtained by excavation.

17/35

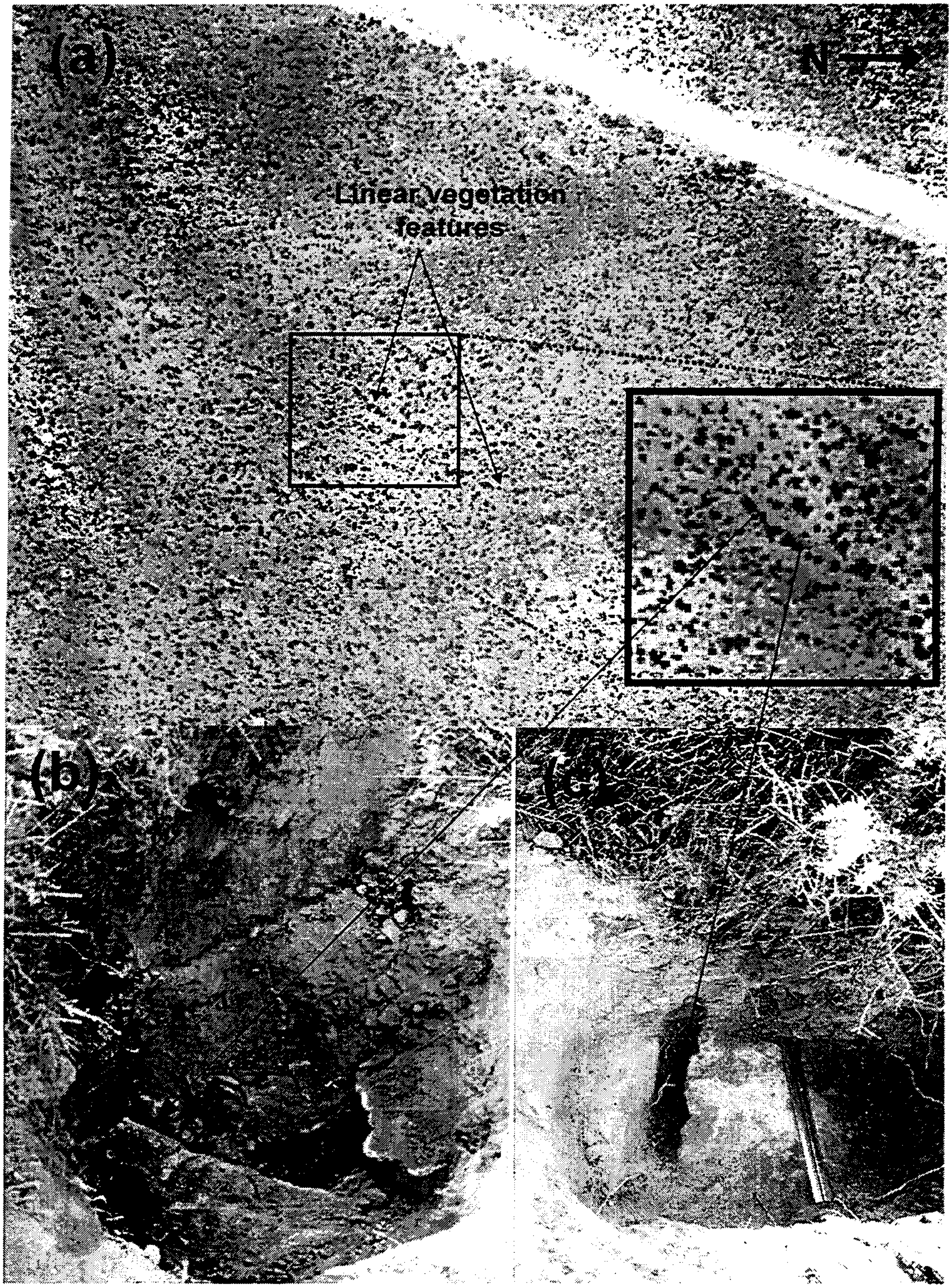

Figure 3-1. Location of a linear vegetation feature in the caprock of Yucca Crest: (a) aerial view, (b) closeup of linear feature, and (c) excavated fissure in bedrock.

4 SIMULATIONS OF ROOT GROWTH INTO FISSURES

4.1 METHODS

The linearity of vegetation features is hypothesized to arise from competitive advantage in the early stages of plant growth, since plants, once established, cannot relocate. To investigate the establishment of vegetation in the presence of shallow soils and bedrock fissures, a 3D simulator was used that explicitly models individual roots, root uptake, and soil water fluxes (version 2.0 of the root-growth simulator (Clausnitzer and Hopmans, 1993, 1994; Somma et al., 1997). These detailed simulations are in part intended to examine the potential applicability of the discrete-root methodology in extrapolating root distributions for future use in more traditional distributed-root models.

A simple test case was used to examine the competitive advantage enjoyed by a seedling located over a soil-filled fissure. The soil is assumed to be uniformly 10 cm in depth, and the fissure is assumed to be 15 cm wide. To ease the computational burden of 3D simulations, symmetry is assumed both perpendicular and parallel to the fissure, so that only half of the fissure is simulated and all side boundaries are represented as no-flow planes. The seedling is germinated in an upper corner of the domain so that one-quarter of a seedling is represented for each simulation; in case 1, the seedling is over the middle of the fissure, while in case 2, the seedling is as far as possible from the fissure. In both cases, the seedling was given an initial leaf area of 2 cm^2 and a single main root, 1.73 cm long, extending diagonally into the domain. A computational grid consisting of elements 2.5 cm on a side was used, with total dimensions of 27.5 × 25 × 200 cm. Soil and bedrock properties are reported in table 4-1.

A number of parameters are required to describe the growth tendencies of a plant, many of which have not been measured for species of interest. Somma et al. (1997) provide estimated parameters that are reasonable for crop plants. In the interest of examining the growth characteristics of a generic plant to identify competitive advantage of fissure growth, most of the provided parameters were not changed, and neither nutrient nor temperature effects on growth were considered changed. Parameters were clearly unreasonable for vegetation adapted to water-stressed environments and were adjusted to achieve less water loss. The parameters used in the simulations are described in table 4-2.

Desert shrubs typically establish viable seedlings only during particularly favorable conditions. In the spirit of examining competitive advantages conveyed to a generic species, favorable conditions were imposed for growth. It was assumed that a thorough rainfall had uniformly brought soil suction head to 0.3 bar (300 cm suction) and bedrock suction head to 3 bar prior to onset of growth. For 15 days, soil water was allowed to redistribute without evapotranspiration (a zero-flux condition for all boundaries), achieving substantially complete equilibrium between soil and bedrock. At the end of the 15 days, the seedling was instantaneously emplaced, and the top boundary was transformed to a specified suction head of 5 bar (5,000 cm) to simulate evaporation. All other boundaries remained zero-flux boundaries at all times. Small rainfall events were simulated at 15, 30, 45, and 75 days by instantaneously increasing the water content to 0.3 at every node in each column of nodes, starting with the top node in the column, until 7.5 mm of water was emplaced for each event. Each column of nodes was filled independently (i.e., lateral flow did not occur during filling).

Table 4-1. Hydraulic parameters for the porous media used in seedling simulation studies

Porous Medium	θ_r (m3m^{-3})	θ_s (m3m^{-3})	α (m^{-1})	n (-)	K_{sat} (m day^{-1})	Maximum Strength[a]
Welded tuff (caprock)[b]	0.002	0.105	0.049	1.43	2.7×10^{-4}	6
Loamy soil[c]	0.078	0.43	3.6	1.56	0.48	10^{11}

[a]Strength at residual saturation was arbitrarily selected, allowing growth in the soil with none in caprock
[b]Retention parameters for sample PW19s; K_{sat} for composite-sample caprock (Flint et al., 1996)
[c]Retention parameters for a loamy soil (Carsel and Parrish, 1988); estimated K_{sat} for Yucca Mountain soil (Schmidt, 1989)

4.2 RESULTS

The root distributions resulting from the two simulations are superimposed in figure 4-1. There is a significant difference between the mass of the two plants, with the plant over the fissure having total root and shoot dry masses of 0.238 g and 0.129 g, respectively, while the plant over the bedrock has total root and shoot dry masses of 0.106 g and 0.065 g, respectively. The plant germinating above the fissure is completely unimpeded by the rock and has extended roots almost 25 cm into the fissure. On the other hand, root growth for the plant above the bedrock is stunted; even lateral growth above the bedrock is inhibited. The plant over the bedrock is, however, able to draw water from the bedrock.

Simulation of water uptake from a set of roots that have grown according to environmental conditions has not been widely explored in the literature, particularly under the constraining conditions of bedrock. The numerical simulation approach is quite time consuming, particularly as the mesh is refined and individual wetting events are considered. The code used for the simulations was designed for agricultural applications, thus the algorithms in the root-growth simulator are designed for soils with relatively smoothly varying strengths. The straightforward explicit algorithm used for growing roots, in which conditions at the root tip (e.g., soil strength, soil strength gradient) determine the size and direction of the root growth, can provide misleading results when there are strong gradients in soil strength such as at material interfaces. In such cases, the explicit algorithm can overshoot physical limits and place the root tip within the rock, where the root is trapped for all subsequent time steps. Two approaches to resolve this difficulty include: (i) adding an additional check for physical plausibility of the new root location; or (ii) providing a gentle transition zone from soil to rock, with the rock material just strong enough to divert the root.

Table 4-2. Parameters describing plant and root growth used in root-growth simulations. Functions are linearly interpolated between extremes and held constant outside of specified ranges.

Parameter	Function	Value
Potential transpiration rate per leaf area	Constant	0.01 cm^3 H_2O cm^{-2} LA hr^{-1}
Dry mass gained per volume of H_2O transpired	Constant	0.0067 g g^{-1}
Leaf area increase per increase in dry shoot mass	Constant	50 $cm^2 g^{-1}$
Root/shoot ratio = f (time)	0 day 15 day	0.6 2.0
Relative stress = f (soil strength)	0 bar 15 bar	0 1
Transpiration multiplier - f (relative stress)	0 1	0.96 0.125
Root/shoot ratio multiplier - f (relative stress)	0 1	0.96 0.125

Axes*		**Order**			
		1	2	3	4
Emergence time (hr)		0	24	120	240
Number of roots started		1	2	2	2
Preferential Growth Angle					
Weighting factor	1	0.95	0.95	0.95	0.95
Maximum random deviation (degree)	1	25	25	25	25

Table 4-2. Parameters describing plant and root growth used in root-growth simulations. Functions are linearly interpolated between extremes and held constant outside of specified ranges. (cont'd)

Branches	Order		
	1	2	3
Unimpeded elongation rate (cm/hr)	0.1	0.02	0.008
Soil strength at which growth ceases (-)	6	6	6
Mass per unit length (gm/cm)			
Soil strength = 0	0.00030	0.00005	0.00001
Soil strength = 6	0.00120	0.00020	0.00004
Sensitivity heading to soil strength	0.1	0.5	1.0
Maximum heading deviation in a root time step (deg)	45	45	45
Maximum branch length (cm)	200	200	200
Branch spacing (cm)	1	0.3	—
Branching angle (deg)	90	90	—
Branching time (hr)	100	150	—

*Roots starting at stem

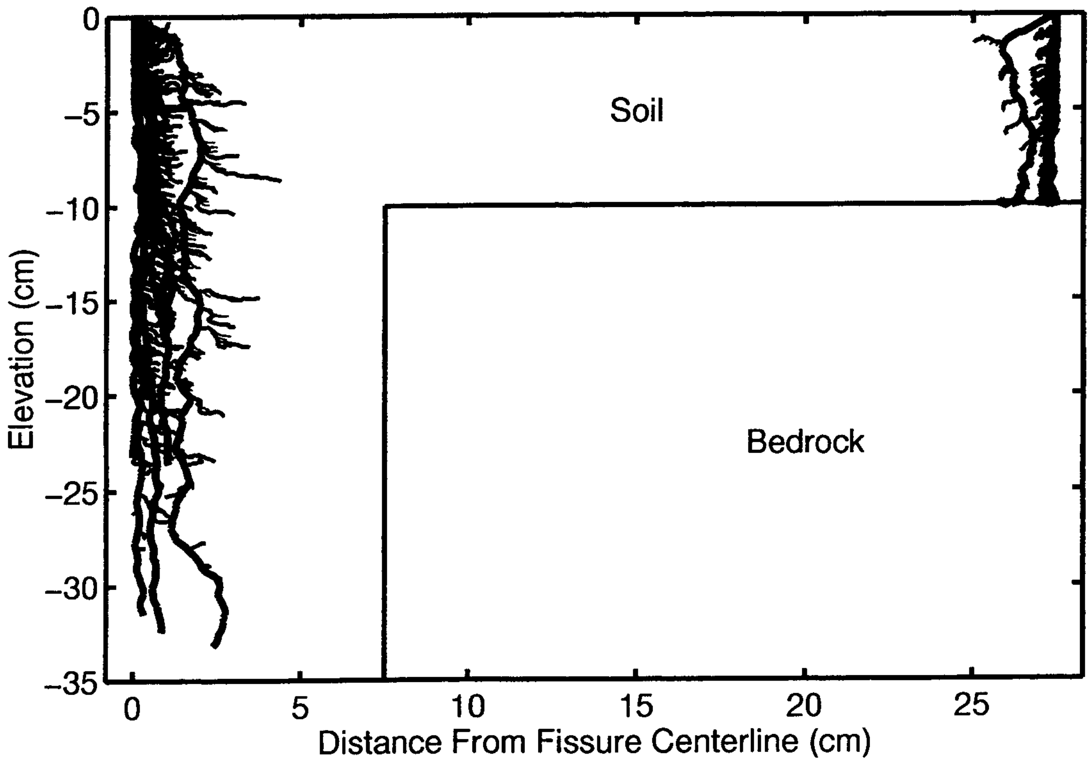

Figure 4-1. Root systems resulting from 100-day growth, overlain into one plot

5 LANDSCAPE-SCALE HYDROLOGIC SIMULATIONS

5.1 METHODS

The HYDRUS-2D model (formerly known as SWMS-2D Šimůnek et al., 1992) was used to simulate the primary hydrologic processes at the landscape scale. The simulation domain represents a vertical 2D cross section (shown in figure 5-1a) derived from the conceptual scheme shown in figure 2-2. Simulation domain dimensions, the finite-element mesh, and material locations are denoted in figure 5-1a. The hydraulic properties for the four types of porous media considered are given in terms of van-Genuchten parameters (van Genuchten, 1980) in table 5-1. The simulation domain includes five vertical fissures in the caprock extending from the caprock surface to an underlying hypothetical fractured-tuff layer. The effective fissure aperture was set to 0.2 m (although 0.1 m may be more typical of the caprock) due to the relatively coarse resolution of the finite-element mesh imposed by computational constraints. There is minimal field evidence supporting the assumption that calcite is present in the bottom of the fissures. Plants were placed over fissures 2, 3, and 5, with relative root distributions depicted in figure 5-1b, to compare hydrologic fluxes in the presence and absence of plant roots within fissures. To examine the role of soil storage capacity, the soil cover increases from upslope to downslope. Fissure 1 represents a scenario in which precipitation falling on exposed bedrock is funnelled into downslope fissures, fissure 5 represents a moderately deep soil cover, and the remaining fissures represent intermediate scenarios.

The system response to different 1 day rainfall-event magnitudes was considered in sets of three simulations: (i) 100 mm, representing an extreme convective summer storm; (ii) 30 mm, representing an average summer thunderstorm; and (iii) 5 mm, representing the intensity and depth of an average winter storm. One set of simulations was performed with no vegetation; a second set considered plant uptake in fissures 2, 3, and 5. The first set of simulations is suggestive of winter conditions, with dormant vegetation, while the second set is suggestive of peak growing season. The boundary conditions for the simulations were: (i) free drainage at the downslope and bottom of the domain, (ii) no flux at the upslope side of the domain, and (iii) atmospheric boundary conditions on the soil surface. At the start of the simulation, a suction head of 5 m (0.5 bar) was applied uniformly throughout the domain. For 4 days prior to the rainfall event, both potential-evaporation rates from the soil surface and potential-transpiration rates allocated over the depth of the roots were assumed to be 2 mm day^{-1}. The rainfall event took place during the fifth day. Subsequent to the rainfall event, the potential-evaporation rate was increased to 3 mm day^{-1}, and the potential-transpiration rate was increased to 4 mm day^{-1} for the reminder of the 35-days simulation.

5.2 RESULTS

Among the six simulations are examples of each significant hydrologic process in the caprock environment under current climatic conditions. The only potentially significant process not found is the relatively unimportant process of overland flow.

One method of assessing the impact of vegetation is to examine the cumulative flux in the fissures. For each of the five fissures, vertical fluxes at centerline nodes at the top of the fissure and at the top of the calcite were tracked. Downward fluxes are negative. For each of the 10 nodes and 6 simulations, the cumulative flux over the 30 days subsequent to the start of rainfall is shown in table 5-2.

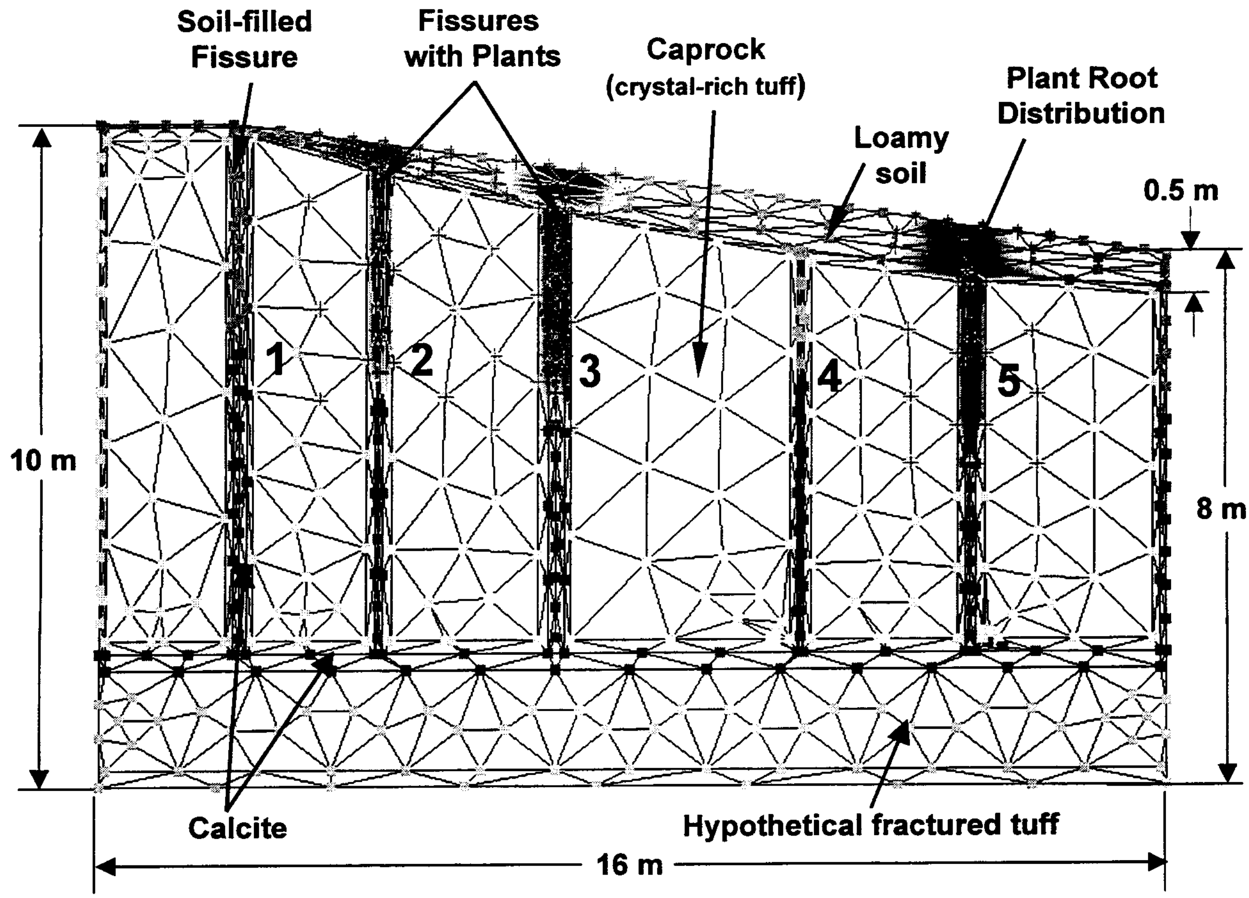

Figure 5-1. Model domain for investigation of flow into fissures

The set of cumulative fluxes in table 5-2 are strikingly suggestive of the potential for transpiring vegetation to reduce net infiltration in this fissured environment. For example, cumulative flux at calcite nodes is upward when plants are in the fissure and downward otherwise. Regardless of the size of the event, the same upward flux occurs. The vegetation has completely prevented the infiltrating water from affecting the calcite, and moreover is drawing water from the calcite. Cumulative downward flux tends to decrease even in fissures not containing plants, which can be attributed to lateral flow due to the presence of vegetation in adjacent fissures.

The 100-mm event represents the largest perturbation to the system and would be most likely to exhibit net infiltration. For this event, the time history of fluxes within each fissure is shown in figure 5-2, which tracks vertical fluxes at the same nodes considered in table 5-2. The effects of lateral flow in the overlying soil upslope of fissure 1, focussing water into fissure 1, can be seen by noting that peak fluxes in figures 5-2a and c are one-third larger than the applied flux for several days after the precipitation event, while fluxes into the other fissures are significantly damped from the applied flux. The strong reduction of flow into those fissures with active plants can also be seen in figures 5-2a and c, while

Table 5-1. Hydraulic parameters for the porous media used in landscape hydraulic simulations studies

Porous Medium	θ_r (m^3m^{-3})	θ_s (m^3m^{-3})	α (m^{-1})	n (-)	K_{sat} (m day^{-1})
Crystal-rich tuff (caprock)[a]	0.045	0.15	0.02	5.0	2.7×10^{-4}
Loamy soil[b]	0.078	0.43	3.6	1.56	3
Calcite (clay)[c]	0.05	0.20	0.8	1.09	0.048
Hypothetical fractured tuff	0.001	0.108	0.28	1.45	0.1

[a]Flint et al. (1996)
[b]Retention parameters for a loamy soil (Carsel and Parrish, 1988) were used to emphasize the role of soil within the fissures (sandy loam to loam).
[c]Retention parameters for a clay (Carsel and Parrish, 1988) were used to emphasize the role of soil within the fissures (sandy loam to loam).

the extraction of soil water from the calcite by plant uptake can be observed by comparison with figures 5-2b and d.

The impact of plant uptake is even more marked in figures 5-3a and c, which suggests that plants can completely shut off influx into fissures for moderate precipitation events. For this smaller event, the wetting pulse due to rainfall reaches a tiny peak at the calcite 3 to 4 weeks after precipitation when no plants are present (most of the flux is due to drainage of the initial conditions). The pulse is swamped by the impact of transpiration. As might be expected, the 5-mm event (not shown) shows no sign of a wetting pulse; evaporation in this system is sufficient to remove the wetting pulse before it reaches the fissure.

Moisture contents 9 days after the 30-mm wetting event are shown in figure 5-4, dramatically demonstrating a result of plant uptake. A small wetting front has penetrated the caprock by several tens of centimeters after 9 days without transpiration. With transpiration, the only caprock location with a wetting front is near the plant-free fissure 4, and the caprock has been desiccated near the plants. By drying the soil and bedrock matrix, plants can create hydraulic barriers in fissures and provide additional soil-water storage to intercept water fluxes.

Plants dynamically regulate uptake, adjusting physiologic requirements to reflect the availability of soil water and seasonal cycles. Over time, plants can adjust their rooting distributions to provide efficient uptake during typical conditions near the plant during periods of active transpiration. Although the simulations presented here are suggestive of how transpiration is potentially able to desiccate the soil and bedrock, adaptive pressures may select plants that limit intake rates so that complete desiccation is not achieved. Such adjustments are not simulated here, but simulations where MAI is of interest over long times may need to account for these adaptive processes.

Table 5-2. Cumulative flux (mm) passing fissure center during the 30 days including and following the rainfall event. Negative values denote downward flux.

Location	Event (mm)	Plant Uptake	Fissure				
			1	2*	3*	4	5*
Top	100	No	−341	−226	−159	−153	−143
Top	100	Yes	−321	−25	−6	−93	−1
Top	30	No	−0.90	−1.43	−2.24	−2.26	−2.26
Top	30	Yes	−1.07	−0.02	−0.02	−1.57	−0.03
Top	5	No	0.83	0.15	−0.44	−0.81	−0.57
Top	5	Yes	0.63	−0.01	−0.02	−0.58	−0.03
Bottom	100	No	−18.2	−8.53	−47.1	−7.83	−10.8
Bottom	100	Yes	−14.6	0.91	0.03	−3.99	0.01
Bottom	30	No	−1.01	−0.94	−2.46	−0.97	−0.98
Bottom	30	Yes	−0.85	0.91	0.03	−0.72	0.01
Bottom	5	No	−0.91	−0.86	−2.20	−0.82	−0.80
Bottom	5	Yes	−0.81	0.91	0.03	−0.64	0.01

*Fissure with plant uptake

The set of simulations presented here demonstrate potential impacts of transpiration. The simulations suggest that net infiltration may be quite small in the caprock environment during the active growing season and exceptional circumstances (e.g., several large storms in a few days, vegetation die-off due to prolonged drought) may be required to cause net infiltration in this season. During the winter, when perennial vegetation is dormant (negligible transpiration), evaporation is minimal, and precipitation is relatively large, the simulations suggest that significant net infiltration can be more easily achieved. Accordingly, most infiltration would be expected during the winter.

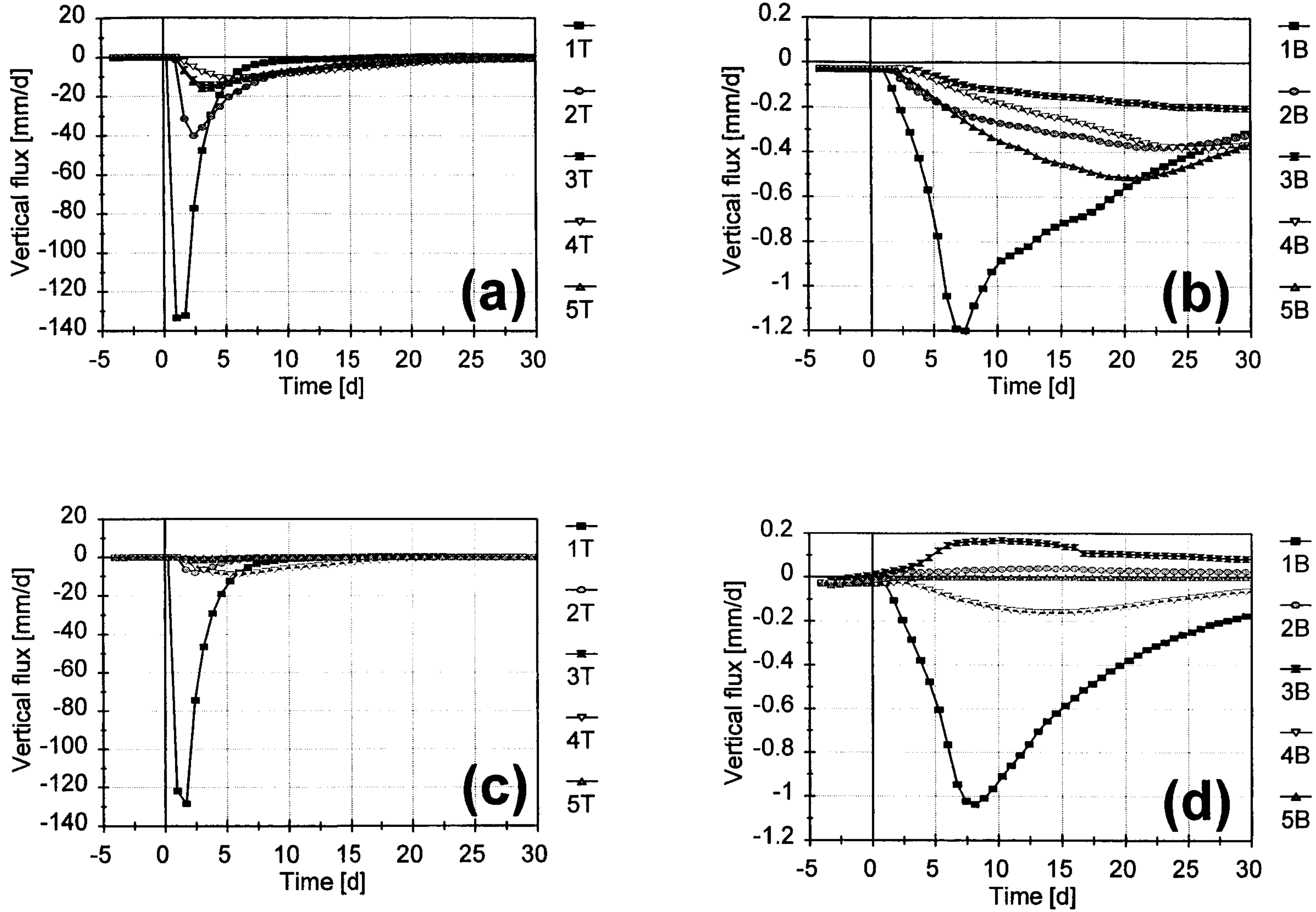

Figure 5-2. Water-flux response in fissures following a 100-mm precipitation event: (a) top of soil filling without plant uptake; (b) bottom of soil filling without plant uptake; (c) top of soil filling with plant uptake, and (d) bottom of soil filling with plant uptake.

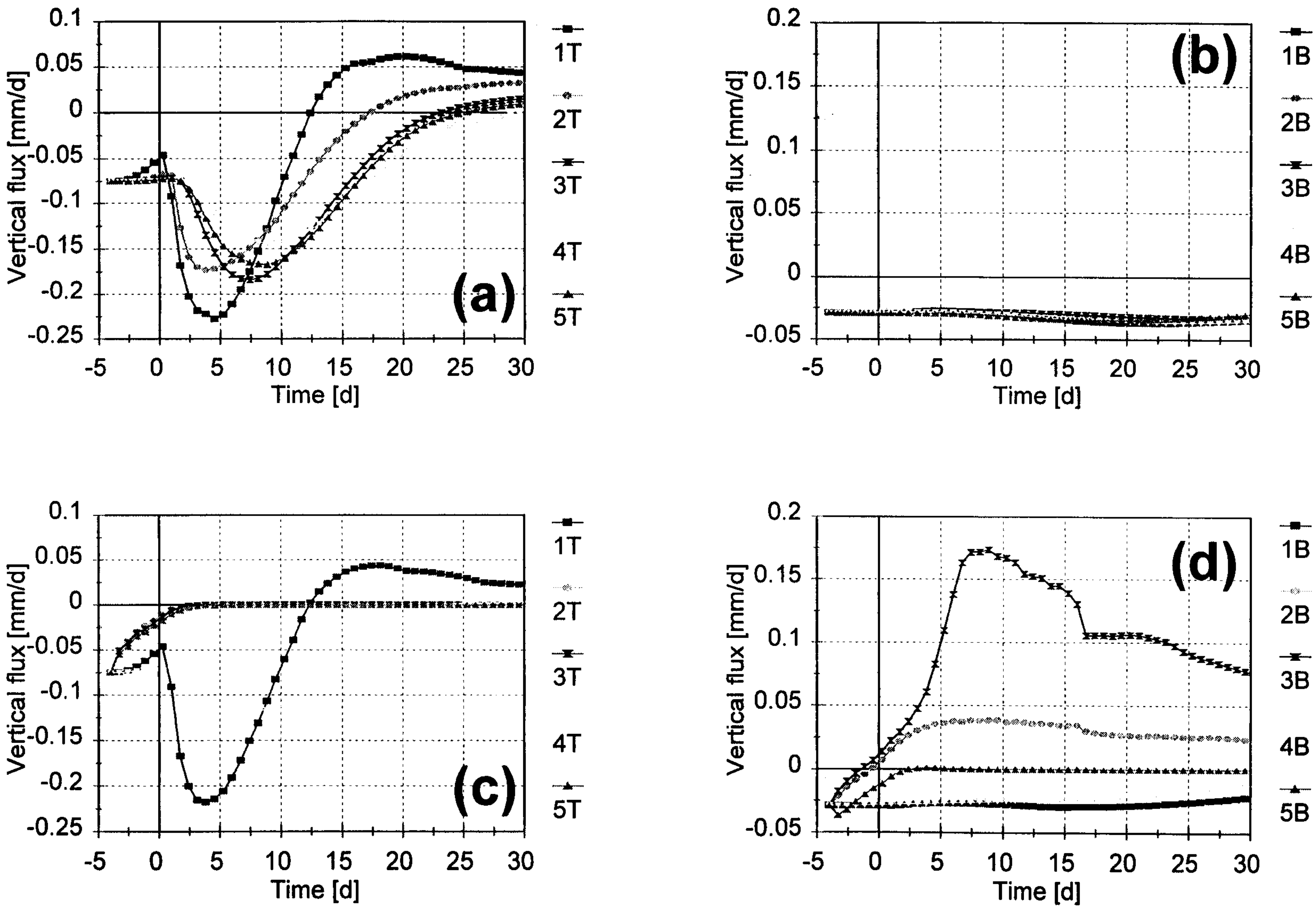

Figure 5-3. Water-flux response in fissures following a 30-mm precipitation event: (a) top of soil filling without plant uptake; (b) bottom of soil filling without plant uptake; (c) top of soil filling with plant uptake; and (d) bottom of soil filling with plant uptake.

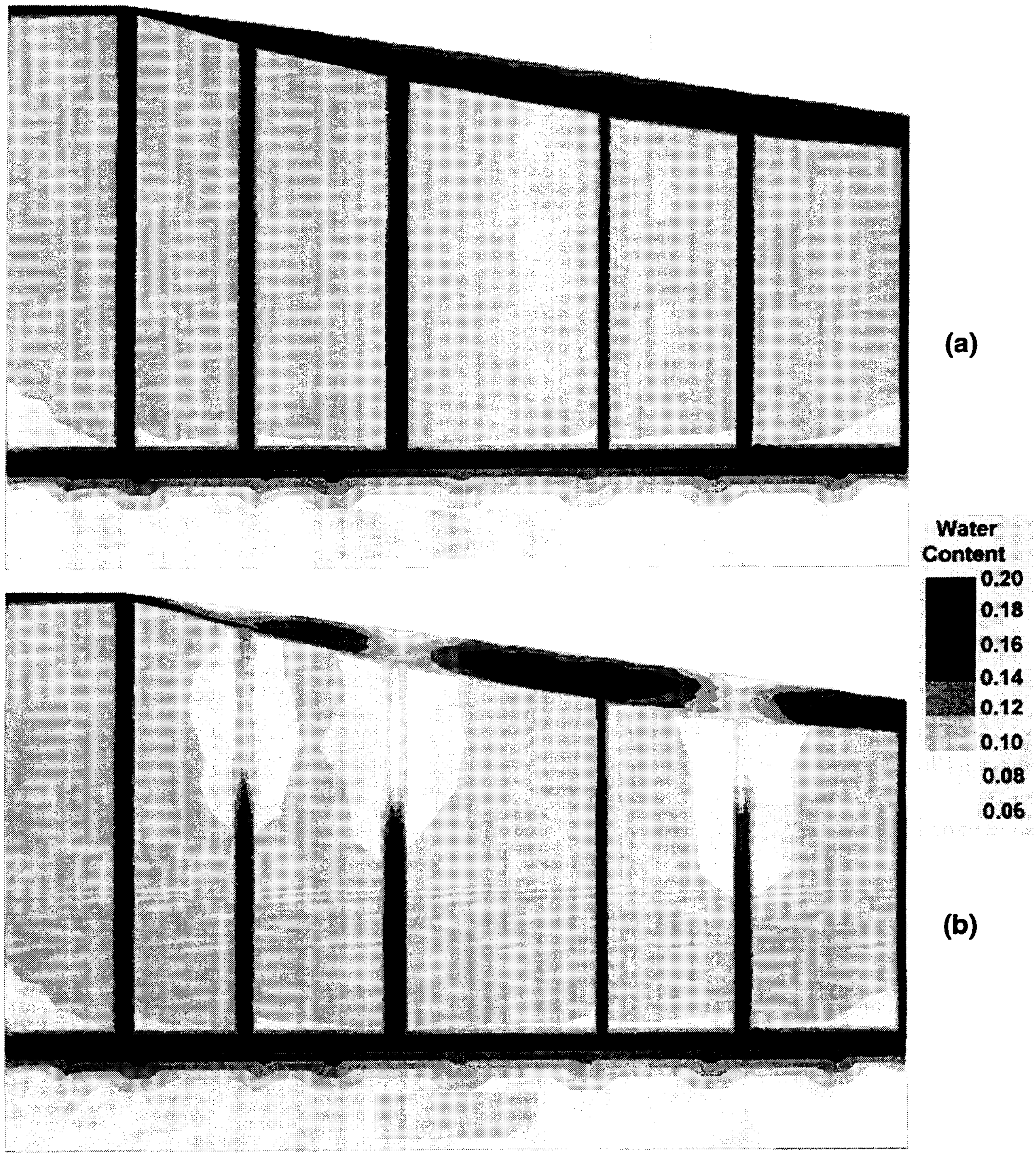

Figure 5-4. Water-content distributions 9 days after a 30-mm rainfall event: (a) without plants, and (b) with plants

30/35

6 SUMMARY AND CONCLUSIONS

Several lines of investigation were used to examine the impact of vegetation upon hydrologic processes in a shallow soil overlying fissured bedrock. Field investigation of perennial vegetation reveals that Great Basin species tend to dominate Mojavean species in the caprock and upper sideslope areas of YM, both in the number of species present and in the total coverage (82 percent of the cover is due to Great Basin species). In general, Great Basin species tend to favor moister and cooler environments than Mojavean species. At YM, Mojavean species were found to dominate only on south-facing slopes with crystal-poor bedrock, which has vegetative cover of 44 percent of corresponding north-facing slopes and 48 percent of the crest (underlain by crystal-rich caprock). The crystal-rich caprock environment is more conducive to plant growth in general than environments underlain by the crystal-poor bedrock, as the vegetative cover in crystal-poor areas with the same general slope and aspect as the caprock environments is only 62 percent of the caprock cover.

Based on field observations, the caprock environment is characterized by shallow aeolian-derived soils (0 to 60 cm in depth) having extremely uniform textures over the potential-repository footprint, widely spaced soil-filled bedrock fissures with apertures possessing widths on the order of 5 to 20 cm, and minimal carbonate deposition except perhaps at depth within the fissures and around rocks within the soil matrix. Soil permeability is large enough to accept the water from most rainfall events without extensive runoff, which is corroborated by a general lack of field evidence for erosive rill formation.

The existence of linear vegetation patterns where the bedrock is covered by soil, readily apparent in low-altitude areal photographs, is one of the striking features of the caprock environment. The exposed root structure of several perennial plants suggests that roots preferentially grow into bedrock fissures unless the soil-water storage capacity of a relatively deep pocket of soil can be exploited. Examination of the root structure for several aligned plants (selected from an areal photograph) where soils are 30 to 60 cm deep revealed a bedrock fissure aligned with the plants, suggesting that bedrock fissures provide a competitive advantage even when the overlying soils are fairly deep.

Hypothesizing that the environment that the plant contacts during early growth exerts the primary control on plant distributions and that the environment atop a fissure is more conducive to plant establishment, a pair of simulations were performed that explicitly considered 3D soil-water redistribution, soil-water uptake by roots, and the growth of individual roots for a hypothetical plant during the early stages after germination. The plant germinating above the fissure had twice the root and shoot mass than the plant germinating 20 cm from the edge of the fissure at the end of the 100-day simulation, supporting the hypothesis. Interestingly, the plant germinating above bedrock was able to extract water from the relatively permeable bedrock, suggesting that the bedrock may form a buffer for plants by quickly storing water during the short period of moist conditions following precipitation and slowly releasing the water over an extended period. Bedrock buffering is also supported by field observations that fine-root growth tends to be especially prolific immediately next to soil/rock interfaces, as also found by (Zwieniecki and Newton, 1995). Without bedrock buffering, it is difficult to provide a mechanism that enables the growth of lateral roots for long enough periods that a root can extend several meters across bedrock with overlying soil depths of only 5 to 10 cm, as can be observed in the field for relatively slow-growing perennial shrubs.

Having established that plants preferentially root within soil-filled fissures in the caprock environment, a set of simulations were performed to examine the hydrologic consequence of plant roots within fissures. The response to precipitation was simulated for (i) a shallow-soil-covered bedrock similar to the caprock

31/35

environment, with three fissures containing plants and two fissures lacking plants; and (ii) an identical set of simulations completely lacking plants. The response to three rainfall amounts was simulated. For the largest storm, fluxes into the calcite filling peaked at 1 to 4 week after the storm when transpiration was not active and were eliminated when fissures had active vegetation. Smaller events enabled additional drainage from the initial conditions by providing additional soil water for evaporation. When plants were active within a fissure, transpiration eliminated net infiltration in the fissure regardless of the size of the storm. The efficacy of transpiration may be partly an artifact of the imposed transpiration rate, which is not based on field measurements.

Two plant-related mechanisms reduced total flux through the plant-filled fissures: (i) transpiration during fissure flow, and (ii) wetting-pulse retardation due to drier fissures prior to rain. The first mechanism appears to be dominant in these simulations.

The impacts of neglecting transpiration and lateral flow were particular concerns raised by Stothoff (1997), who considered MAI for shallow soils over a fracture continuum under bare-soil conditions using one-dimensional (1D) simulations. Stothoff (1997) found that simulated bare-soil MAI decreased roughly as a power of the soil depth when depths were shallow, qualitatively consistent with the results presented here for the 100-mm event without plants. The simulations presented by Stothoff (1997) tend to have most net infiltration occurring in the winter, with evaporation alone generally effective at eliminating net infiltration at other times. Use of 1D approximation implies that suction heads are identical laterally. The simulations presented here, although not exhaustive, do suggest that lateral redistribution rapid equilibrates suction heads, supporting the 1D approximation at least when vegetation is dormant.

The various lines of investigation discussed in this paper all suggest that fissures have a dominant effect on recharge processes within the shallow-soil-covered caprock environment. Vegetation, dependent on soil-water availability, strongly shows the influence of fissures. Root-growth simulations suggest that vegetation should have a strong preference for growing into fissures, and flow simulations also suggest that there should be strongly focussed flow into fissures. Despite the complexity of modeling this environment, several factors are conducive to relatively robust predictions of MAI. The caprock environment, hydrologic soon after a rainfall is characterized large fluxes when flow is occurring, rapid removal of water to below the rooting zone, relatively low impact of vegetation during events that generate net infiltration, and long hiatuses between flow events. Deep alluvium also has long hiatuses between flow events, but subsurface flows are generally slower, due to relatively large soil-water storage and it is more difficult for infiltrating water to move below the rooting zone before plants can take up the water.

Although flow processes in deep alluvium have been better characterized in the literature than in shallow soils, the relatively large and discrete net-infiltration events in shallow soils (with limited plant uptake) may make predictions of MAI in shallow soils more robust than predictions in deep alluvium. The robustness of predictions in shallow soils derives from the diminished sensitivity to small errors during these large events. French et al. (1996) observe the net infiltration events on the Nevada test site only occur for precipitation events above a threshold level, and that the frequency and magnitude of these events can be predicted. Applying this observation to the caprock environment, MAI might be robustly predicted by only performing simulations for those few events that might case significant net infiltration.

7 REFERENCES

Allison, G.B., and M.W. Hughes. 1978. The use of environmental chloride and tritium to estimate total recharge to an unconfined aquifer. *Australian Journal of Soil Research* 16: 181–195.

Allison, G.B., G.W. Gee, and S.W. Tyler. 1994. Vadose-Zone techniques for estimating groundwater recharge in arid and semiarid regions. *Soil Science Society of America Journal* 58(1): 6–14.

Andrews, R.W., T.F. Dale, and J.A. McNeish. 1994. *Total System Performance Assessment—1993: An Evaluation of the Potential Yucca Mountain Repository.* B00000000-01717-2200-00099-Rev.01, Las Vegas, NV: Intera, Inc.

Bagtzoglou, A.C., N.M. Coleman, E.C. Pearcy, S.A. Stothoff, and G.W. Wittmeyer. 1996. *Unsaturated and Saturated Flow Under Isothermal Conditions.* B. Sagar, ed. NRC High-Level Radioactive Waste Program FY96 Annual Progress Report, Volume NUREG/CR-6513, No. 1, Washington, DC: Nuclear Regulatory Commission.

Barnes, C.J., G. Jacobson, and G.D. Smith. 1994. The distributed recharge mechanism in the australian arid zone. *Soil Science Society of America Journal* 58(1): 31–40.

Buesch, D.C., R.W. Spengler, T.C. Moyer, and J.K. Geslin. 1996. *Proposed Stratigraphic Nomenclature and Macroscopic Identification of Lithostratigraphic Units of the Paintbrush Group Exposed at Yucca Mountain, Nevada.* Open-File Report 94-469. Denver, CO: United States Geological Survey.

Campbell, G.S. 1985. *Soil Physics with BASIC.* Amsterdam, Netherlands. Elsevier Science Publisher B.V.

Carsel, R.F., and R.S. Parrish. 1988. Developing joint probability distributions of soil water retention characteristics. *Water Resources Research* 24(5): 755–769.

Clausnitzer, V., and J.W. Hopmans. 1993. *An Algorithm for Three-Dimensional, Simultaneous Modeling of Root Growth and Transient Soil Water Flow, V 1.0.* LAWR Paper No. 100022, Department of Land, Air, and Water Resources. Davis, CA: University of California.

Clausnitzer, V., and J.W. Hopmans. 1994. Simultaneous modeling of transient three-dimensional root growth and soil water flow adaptation. *Plant and Soil* 164: 299–314.

Conrad, S.H. 1993. Using Environmental Tracers to Estimate Recharge Through an Arid Basin. *In Proceedings of the Fourth Annual High Level Radioactive Waste Management Conference.* La Grange Park, IL: American Nuclear Society. 132–137.

Electric Power Research Institute. 1990. *Demonstration of a Risk-Based Approach to High-Level Waste Repository Evaluation.* EPRI NP-7057. Palo Alto, CA: Electric Power Research Institute.

Electric Power Research Institute. 1992. *Demonstration of a Risk-Based Approach to High-Level Waste Repository Evaluation: Phase 2.* EPRI TR-100384. Palo Alto, CA: Electric Power Research Institute.

33/35

Electric Power Research Institute. 1996. *Yucca Mountain Total System Performance Assessment, Phase 3*. EPRI TR-107191. Palo Alto, CA: Electric Power Research Institute.

Eslinger, P.W., L.A. Doremus, D.W. Engel, T.B. Miley, M.T. Murphy, W.E. Nichols, M.D. White, D.W. Langford, and S.J. Ouderkirk. 1993. *Preliminary Total-System Analysis of a Potential High-Level Nuclear Waste Repository at Yucca Mountain*. PNL-8444. Richland, WA. Pacific Northwest Laboratory.

Evans, D.D., T.W. Sammis, and D.R. Cable. 1981. Actual Evapotranspiration under Desert Conditions. D.D. Evans and J. Thames, eds. *Water in Desert Ecosystems*. 195–218

Fabryka-Martin, J.T., H.J. Turin, A.V. Wolfsberg, D. Brenner, P.R. Dixon, and J.A. Musgrave. 1996. *Summary Report of Chlorine-36 Studies*. LA-CST-TIP-96-003. Los Alamos, NM: Los Alamos National Laboratory.

Fayer, M.J., and T.L. Jones. 1990. *UNSAT-H Version 2.0: Unsaturated Soil Water and Heat Flow Manual*. PNL-6779. Richland, WA: Pacific Northwest Laboratory.

Flint, A. L., J.A. Hevesi, and L.E. Flint. 1996. *Conceptual and Numerical Model of Infiltration for the Yucca Mountain Area, Nevada*. Milestone 3GUI623M. Las, Vegas, NV: Department of Energy.

Flint, L.E. 1996. *Matrix Properties of Hydrogeologic Units at Yucca Mountain, Nevada*. Milestone 3GUP604M. Las Vegas, NV: Department of Energy

Flint, L.E., and A.L. Flint. 1995. *Shallow Infiltration Processes at Yucca Mountain, Nevada—Neutron Logging Data 1984-93*. Water-Resources Investigations Report 95-4035, Denver, CO: U.S. Geological Survey.

Flint, L.E., A.L. Flint, and J.A. Hevesi. 1994. Shallow infiltration processes in arid watersheds at Yucca Mountain, Nevada. *In Proceedings of the Fifth Annual High Level Radioactive Waste Management Conference*. La Grange Park, IL: American Nuclear Society: 2,315–2,322.

Flint, L.E., A.L. Flint, C.A. Rautman, and J.D. Istok. 1996. *Physical and Hydrologic Properties of Rock Outcrop Samples at Yucca Mountain, Nevada*. Open-File Report 95-280. Denver, CO: U.S. Geological Survey.

Fonteyn, P.J., and B.E. Mahall. 1981. An experimental analysis of structure in a desert plant community. *Journal of Ecology* 69: 883–896.

French, R., R. Jacobson, and B. Lyles. 1996. Threshold precipitation events and potential ground-water recharge. *Journal of Hydraulic Engineering* 122 (10): 573–578.

Gee, G.W., P.J. Wierenga, B.J. Andraski, M.H. Young, M.J. Fayer, and M.L. Rockhold. 1994. Variations in water balance and recharge potential at three western desert sites. *Soil Science Society of America Journal* 58(1): 63–72.

Gerwitz, A., and E.R. Page. 1974. An empirical mathematical model to describe plant root systems. *Journal of Applied Ecology* 11: 773–782.

34/35

Goodall, D.W. 1952. Some considerations in the use of point quadrats for the analysis of vegetation. *Australian Journal of Scientific Research* 5: 1–41.

Groeneveld, D.P. 1997. Vertical point quadrat sampling and an extinction factor to calculate leaf area index. *Journal of Arid Environments*. (In press).

Heady, J.F., R.P. Gibbens, and R.W. Powell. 1959. A comparison of the charting, line intercept and line-point methods of sampling shrub types of vegetation. *Journal of Range Management* 12: 180–188.

Herwitz, S.R., and L. Olsvig-Whittaker. 1989. Preferential upslope growth of Zygophyllum dumosum Boiss. (Zygophyllaceae) roots into bedrock fissures in the northern Negev desert. *Journal of Biogeography* 16: 457–460.

Hickman, J.C. 1995. *The Jepson Manual of Higher Plants of California*. Berkeley, CA: University of California Press.

Leary, K.D. 1990. *Analysis of techniques for estimating potential recharge and shallow unsaturated zone water balance near Yucca Mountain, Nevada*. Master's thesis, University of Nevada.

Long, A. and S.W. Childs. 1993. Rainfall and Net Infiltration Probabilities for Future Climate Conditions at Yucca Mountain. *In Proceedings of the Fourth Annual High Level Radioactive Waste Management Conference*. La Grange Park, IL: American Nuclear Society. 112–121.

Nichols, W.D. 1987. *Geohydrology of the Unsaturated Zone at the Burial Site for Low-Level Radioactive Waste Near Beatty, Nye County, Nevada*. Water-Supply Paper 2312. Denver, CO: U.S. Geological Survey.

Noy-Meir, I. 1973. Desert ecosystems: Environment and producers. *Annual Review of Ecological Systems* 4: 25–52.

Nuclear Regulatory Commission. 1992. *Initial Demonstration of the NRC's Capability to Conduct a Performance Assessment for a High-Level Waste Repository*. NUREG-1327. Washington, DC: Nuclear Regulatory Commission.

Nuclear Regulatory Commission. 1995. *NRC Iterative Performance Assessment Phase 2: Development of Capabilities for Review of a Performance Assessment for a High-Level Waste Repository*. NUREG-1464. Washington, DC: Nuclear Regulatory Commission.

Phillips, F.M. 1994. Environmental tracers for water movement in desert soils of the american southwest. *Soil Science Society of America Journal* 58(1): 15–24.

Quade, J., and T.E. Cerling. 1990. Stable isotopic evidence for a pedogenic origin of carbonates in trench 14 near Yucca Mountain, Nevada. *Science* 250: 1,549–1,552.

Ratliff, L.F., J.T. Ritchie, and D.K. Cassel. 1983. Field-measured limits of soil water availability as related to laboratory-measured properties. *Soil Science Society of America Journal* 47: 770–775.

35/35

Sandia National Laboratories. 1992. *Total-System Performance Assessment 1991: An Initial Total-System Performance Assessment for Yucca Mountain*. SAND91-2795. Albuquerque, NM: Sandia National Laboratories.

Sandia National Laboratories. 1994. *Total-System Performance Assessment for Yucca Mountain—SNL Second Iteration (TSPA-1993)*. SAND93-2675. Albuquerque, NM: Sandia National Laboratories.

Sass, J. H., A.H. Lachenbruch, W.W. Dudley, Jr., S.S. Priest, and R.J. Munroe. 1988. *Temperature, thermal conductivity, and heat flow near Yucca Mountain, Nevada: Some tectonic and hydrologic implications*. Open-File Report 87-649. Denver, CO: U.S. Geological Survey.

Scanlon, B.R. 1991. Evaluation of moisture flux from chloride data in desert soils. *Journal of Hydrology* 128: 137–156.

Scanlon, B.R. 1992. Evaluation of liquid and vapor water flow in desert soils based on chlorine 36 and tritium tracers and nonisothermal flow simulations. *Water Resources Research* 28(1): 285–297.

Schmidt, M.R. 1989. *Classification of Upland Soils by Geomorphic and Physical Properties Affecting Infiltration at Yucca Mountain, Nevada*. Master's thesis, Colorado State University.

Šimůnek, J., T. Vogel, and M.T. van Genuchten. 1992. *The SWMS_2D code for simulating water flow and solute transport in two-dimensional variably saturated media V. 1.1*. Research Report No. 126. Riverside, CA U.S. Salinity Laboratory.

Somma, F., V. Clausnitzer, and J.W. Hopmans. 1997. *An Algorithm For Three-Dimensional, Simultaneous Modeling Of Root Growth, Transient Soil Water Flow, And Solute Transport And Uptake, Version 2.1*. LAWR Paper No. 100034. Department of land, Air and Water Resources. Davis, CA: University of California.

Stephenson, N.L. 1990. Climate control of vegetation distribution: The role of the water balance. The *American Naturalist* 135: 649–670.

Stothoff, S.A. 1997. Sensitivity of long-term bare soil infiltration simulations to hydraulic properties in an arid environment. *Water Resources Research* 33(4): 547–558.

TRW Environmental Safety Systems, Inc. 1995. *Total System Performance Assessment--1995: An Evaluation of the Potential Yucca Mountain Repository*. B00000000-01717-2200-00136. Las Vegas, NV. TRW Environmental Safety Systems Inc.

Tyler, S.W., and G.R. Walker. 1994. Root zone effects on tracer migration in arid zones. *Soil Science Society of America Journal* 58(1): 25–31.

van Genuchten, M.T. 1980. A closed-form equation for predicting the hydraulic conductivity of unsaturated soils. *Soil Science Society of America Journal* 44: 892–898.

Zwieniecki, M.A., and M. Newton. 1995. Roots growing into rock fissures: Their morphological adaptation. *Plant and Soil* 172: 181–187.